JPET Fast Forward. Published on January 8, 2018 as DOI: 10.1124/jpet.117.243493
This article has not been copyedited and formatted. The final version may differ from this version.

1. Title page

Dual blockade of interleukin-1β and interleukin-17A reduces murine arthritis pathogenesis but also leads to spontaneous skin infections in non-human primates†

Authors:

Melanie C. Ruzek*, Lili Huang, Ting Ting Zhang, Shaughn Bryant, Peter F. Slivka, Carolyn A. Cuff, Catherine Tripp and Guenter Blaich

Author Affiliations:

AbbVie Inc. Bioresearch Center 100 Research Dr., Worcester, MA 01605 (MCR, LH, TTZ, SB, PS, CC,)

AbbVie Deutschland GmbH & Co KG, Knollstrasse, 67061, Ludwigshafen, Germany (GB)

Former Abbvie employee (CT)

Primary Laboratory of Origin:

Abbvie Bioresearch Center

100 Research Drive

Worcester, MA 01605

2. Running Title Page

Spontaneous infection in monkeys with IL-1β/IL-17A blockade

Corresponding author:

Melanie C Ruzek

Abbvie Bioresearch Center

100 Research Drive

Worcester, MA 01605

508-688-3330

Melanie.ruzek@abbvie.com

Number of pages: 52

Number of tables: 5

Number of figures: 6

Number of references: 30

Number of words in Abstract: 250

Number of words in Introduction: 364

Number of words in Discussion: 1402

List of non-standard abbreviations: RA, rheumatoid arthritis; IL, interleukin; G-CSF, granulocyte colony stimulating factor; CXCL, CXC chemokine ligand; DVD-Ig, dual variable domain immunoglobulin; ABBV-615, anti-IL-1β/IL-17A DVD-Ig; LCN2, lipocalin 2; TNF, tumor necrosis factor; Th, T helper; KO, knock-out; S100A8/9, S100 calcium binding proteins

JPET Fast Forward. Published on January 8, 2018 as DOI: 10.1124/jpet.117.243493
This article has not been copyedited and formatted. The final version may differ from this version.

A8 or A9; CIA, collagen induced arthritis; IC_{50}, 50% inhibitory concentration; GLP, good laboratory practice; CL, clearance; V, volume of distribution; C_{max}, maximal concentration; $AUC_{0\text{-}168h,}$ area under the concentration-time curve from time 0-168hrs; ADA, anti-drug antibodies; SPR, surface plasmon resonance; ANOVA, analysis of variance

Recommended section assignment: Inflammation, Immunopharmacology and Asthma

JPET Fast Forward. Published on January 8, 2018 as DOI: 10.1124/jpet.117.243493
This article has not been copyedited and formatted. The final version may differ from this version.

3. Abstract

Despite the efficacy of biologics for treatment of rheumatoid arthritis (RA), many patients show inadequate responses and likely require neutralization of multiple mediators. Neutralization of both interleukin (IL)-1β and IL-17A with monoclonal antibodies showed greater efficacy than either agent alone in a mouse arthritis model with cooperative inhibition of key inflammatory factors, IL-6, granulocyte colony stimulating factor (G-CSF) and CXC chemokine ligand (CXCL)1. Given the potential clinical benefit in RA, we generated a human dual variable domain antibody (DVD-Ig), ABBV-615, capable of simultaneous binding and neutralization of IL-1β and IL-17A. ABBV-615 was characterized and evaluated in cynomolgus monkeys for pharmacokinetics and toxicity to enable clinical development. ABBV-615 exhibited affinities (K_D) of 12 and 3 pM on human IL-1β and IL-17A, respectively, and potencies (IC_{50}) of 3 and 58 pM, respectively, as well as excellent drug-like properties. ABBV-615 pharmacokinetics in cynomolgus monkeys was dose proportional from 20 to 100 mg/kg with a mean half-life of 16d. However, a 13-week repeat-dose toxicity study in cynomolgus monkeys revealed time-dependent spontaneous infections exclusively in skin at all doses tested and not historically seen with single agent anti-IL-1α/β or anti-IL-17A. Consistent with reduced resistance to skin infections, IL-1β and IL-17A-stimulated human keratinocytes demonstrate cooperative or compensatory production of key anti-bacterial and inflammatory mediators such as Lipocalin-2 (LCN2), G-CSF, CXCL1, IL-8, tumor necrosis factor (TNF) and IL-6, which aid in defense against skin bacterial infections. These results illustrate the skin-specific antimicrobial mechanisms of IL-1β and IL-17A and highlight the importance of understanding unique combinatorial effects of biological agents.

JPET Fast Forward. Published on January 8, 2018 as DOI: 10.1124/jpet.117.243493
This article has not been copyedited and formatted. The final version may differ from this version.

4. Introduction

While there have been significant advancements made in the treatment of autoimmune diseases such as rheumatoid arthritis (RA), a number of patients remain partially responsive or unresponsive to therapy. In an attempt to address this unmet need, we generated an anti-IL-1β/IL-17A dual-variable domain Ig molecule to concomitantly neutralize IL-1β and IL-17A, both of which are involved in RA disease pathophysiology (Mateen et al. 2016).

IL-1α and β (IL-1) are proinflammatory cytokines that drive innate immune responses by inducing chemokines and cytokines to activate and recruit immune cells, thereby promoting inflammation. In addition, IL-1 stimulates adaptive immune responses by activating and promoting T helper (Th)17 cells, which produce IL-17A, among other cytokines. IL-17A stimulates chemokine production to recruit neutrophils and other immune cells to sites of inflammation. In support of their role in inflammation, blockade of IL-1 or IL-17A shows significant efficacy in autoinflammatory syndromes and psoriasis, respectively (Jesus and Goldbach-Mansky, 2014; Canavan et al., 2016). Both IL-1 and IL-17A have been suggested to contribute to RA pathogenesis through induction of other proinflammatory cytokines from fibroblasts and monocytes, recruitment of other immune cells, as well osteoclast activation, osteoclastogenesis and cartilage damage (Choy et al. 2012). Single agent IL-17A and IL-1 antagonists were only modestly effective (Alten, et al., 2011, Cohen, et al., 2004, Cardiel, et al., 2010, Genovese, et al., 2013) in RA, but leave open the possibility for superior combinatorial effects. The potential combinatorial effects of dual IL-17A and IL-1β targeting has been suggested in mouse models where treatment with anti-IL-17A and anti-IL-1β neutralizing antibodies or a bispecific anti IL-1/IL-17A antibody resulted in a greater reduction in severity of arthritis, bone damage and cartilage destruction (Zhang, et al. 2013, Wu, et al.

2016). A separate study evaluating anti-IL-17A treatment of IL-1-deficient human transgenic TNF mice also impaired the spontaneous development of arthritis to a greater degree than anti-IL-17A treatment or IL-1 deficiency alone (Zwerina, et al., 2012).

These present studies confirm and extend upon the combinatorial efficacy of anti-IL-1β and IL-17A in a mouse arthritis model, describe the generation and characterization of an anti-IL-1β/IL-17A DVD-Ig molecule, ABBV-615, and testing of this agent in a repeat-dose cynomolgus monkey toxicology study to determine feasibility for clinical development.

JPET Fast Forward. Published on January 8, 2018 as DOI: 10.1124/jpet.117.243493
This article has not been copyedited and formatted. The final version may differ from this version.

5. Methods

Collagen-induced arthritis mouse study

Male DBA/1J mice were obtained from Jackson Labs (Bar Harbor, ME) and used at 6 to 8 weeks of age. All procedures were performed in accordance with the Guide for the Care and Use of Laboratory Animals as adopted and promulgated by the U.S. National Institutes of Health as well as the Institutional Animal Care and Use Committee and monitored by an attending veterinarian.

Type II Bovine Collagen was obtained from MD Biosciences, Inc. (St.Paul, MN). Zymosan A was obtained from Sigma (St. Louis, MO). Surrogate mouse mAbs for anti-IL-1β and anti-IL-17A were used in the mouse model. Mouse anti-human IL-17A IgG2a/k mAb (1D10) was produced at AbbVie in an HEK-293-6E cell line utilizing Entrez human gene sequence 3605 as this mAb showed significant cross-reactivity to and neutralization of mouse IL-17A. Mouse anti-mouse IL-1β IgG2a/k mAb (10G11.B11) was prepared at Harlan Bioproducts (Indianapolis, IN) utilizing Entrez mouse gene sequence 16176.

Arthritis was induced with an intradermal (i.d.) injection at the base of the tail with 100µl emulsion containing 100 µg of type II bovine collagen in 0.1N acetic acid and 100µL of complete Freund's adjuvant containing 100 µg of Mycobacterium tuberculosis H37Ra (BD Difco, Franklin Lakes, NJ). A boost of 1.0 mg zymosan A in 200 µL of phosphate buffered saline (Life Technologies, Grand Island, NY) was given 21 days later intra-peritoneally (i.p.). Disease onset occurred within 3-7 days following the boost and mice were monitored daily for a change in paw swelling with a caliper thickness-gage (310-115, Dyer Co, Lancaster, PA). Mice were enrolled for the study between days 24 and 28 at the first clinical signs of disease

and treated with 5 mg/kg anti IL-1β and 12 mg/kg anti-IL-17A twice a week by i.p. injection, which were previously established maximally efficacious doses in this model (data not shown). At the termination of the experiment serum was collected for mAb exposure and paws were collected for histopathology or homogenization for mRNA or cytokine/chemokine protein analysis.

For histopathological evaluation, left and right rear paws were fixed in neutral buffered formalin, decalcified in Cal-Rite, routinely processed in paraffin, sectioned and stained with hematoxylin and eosin. All joints in each paw section were evaluated and the paw was assigned a total score for synovial cell proliferation/cellular infiltrates (pannus), cartilage damage and bone erosion by a board-certified veterinary pathologist. Slides were scored blinded as follows: 0=No significant lesion, 1=Minimal, 2=Mild, 3=Moderate, 4=Severe. A total of 26 animals per group were evaluated for paw swelling and 10 animals per group were evaluated by histological scoring A two-way ANOVA with Bonferroni post test was used to determine statistical significance.

Paws for homogenization for either protein or RNA analysis were frozen immediately in liquid nitrogen and stored at –80^{o}C until processing. For protein analysis, tissues were pulverized frozen with a Bio-Pulverizer (BioSpec Products, Inc, Bartlesville, OK), and transferred to Bullet Blender Bead Lysis tubes (Next Advance, Inc, Averill Park, NY) on water-ice. Ice-cold 750 µL of radioimmunoprecipitation assay lysis buffer (RIPA) containing a Protease Inhibitor Cocktail for use with mammalian cell and tissue extracts (Sigma) was added to each tube and homogenized twice using a bullet blender at maximum speed, for 30 s each. Once homogenized, tubes were spun for 10 min at 10,000 G and the supernatant is removed to a 96-well plate for analysis. Cytokines and chemokines were analyzed by MesoScale Discovery

(Rockville, MD) electro-chemiluminescence (Mouse ProInflammatory 7-Plex Kit). For gene expression analysis, paws were first pulverized on dry ice and bone fragments were placed into Qiazol (Qiagen, Germantown, MD) and refrozen. A standard chloroform extraction and isopropanol precipitation was performed to isolate the RNA. Total RNA was converted to cRNA using the Affymetrix 3'IVT labeling kit and 10μg of IVT product was hybridized onto the gene strip array according to the manufacturer's protocol (Affymetrix, Santa Clara, CA). Raw data was converted to expression in Expression Console (Affymetrix) and imported into Excel for additional analysis. Three to four animals per group were assessed for gene expression analyses and five animals per group for paw homogenate protein. Statistical significance was determined with a one-way ANOVA with Bonferroni post-test.

Generation of ABBV-615

ABBV-615, also known as DVD3418, is a potent human anti-IL-1β/IL-17A DVD-Ig that was engineered from mAbs to human IL-1β and IL-17A. The design and generation of DVD-Igs were carried out as previously described (Wu et al., 2007; Lacy et al. 2015). Briefly, the two variable domains of the anti-IL-1β mAb and the anti-IL-17A mAb were fused in frame with glycine-serine peptide linkers in each DVD-Ig heavy chain (HC) and light chain (LC) using overlapping polymerase chain reaction (PCR). The PCR products encoding DVD-Ig HC and LC were subcloned into mammalian expression vectors. ABBV-615 protein was generated by transient transfection of HEK 293-6E cells with HC- and LC-expressing plasmids or in a CHO cell line stably expressing ABBV-615, and purified by protein A sepharose affinity chromatography. In ABBV-615, the anti-IL-1β variable domain is at the 5'-end as the outer domain and the anti-IL-17A variable domain is at the 3'-end as the inner domain. ABBV-615 is a human IgG1 with mutations in the Fc region (L234A, L235A) (based on EU numbering

system) that impair its effector function by reducing interaction with complement and human Fcγ receptors.

Binding Affinity Measurement of ABBV-615 by Surface Plasmon Resonance

The binding affinities of ABBV-615 to IL-1β and IL-17A from human, cynomolgus monkey (Macaca fascicularis), rabbit, rat and mouse were determined by surface plasmon resonance (SPR) analysis using Biacore T200 instrument (Serial Number 1464285, GE Healthcare Life Sciences, Piscataway, NJ). ABBV-615 was captured by a goat anti-human IgG Fc polyclonal antibody (Thermo Scientific, Waltham, MA) that was covalently immobilized across a CM5 biosensor chip via amino groups. Serially diluted cytokine solutions (human IL-1β and IL-1β species at 0.39-50 nM, human IL-17A at 0.78-100 nM, and IL-17A species at 0.195-200 nM) were injected at a flow rate of 50 µL/min. After a dissociation step, surface was regenerated with 10 mM Glycine, pH 1.5, at 100 µL/min. Association and dissociation rate constants, as well as overall affinity (equilibrium dissociation constant K_D) were calculated by the instrument evaluation software based on the values extracted from the data using global fit analysis.

Sequential Binding of IL-17A and IL-1β to ABBV-615 by Surface Plasmon Resonance

ABBV-615 was captured by the goat anti-human IgG Fc polyclonal antibody (pAb) immobilized on CM5 chip. IL-17A and IL-1β, both at 200 nM, were injected sequentially to attain saturation. Then the experiment was repeated in the reverse order of sequential injection of the cytokines. Surfaces were regenerated with 10 mM Glycine, pH 1.5 at a flow rate of 100 µL/min. Binding stoichiometry was calculated according to GE Healthcare guidelines utilizing binding response signals and respective molecular weights of the molecules.

Bioassays for determination of ABBV-615 neutralization potency

ABBV-615 was tested *in vitro* for its IL-1β and IL-17A neutralization activity by IL-1β bioassay and IL-17A bioassay, respectively. Neutralization of human, cynomolgus monkey, and rabbit IL-1β by ABBV-615 was measured in an IL-8 release assay in a human fetal lung fibroblast cell line MRC-5 (ATCC, Manassas, VA) which produces IL-8 in response to human or cynomolgus monkey IL-1β, as described previously (Wu et al., 2007; Lacy et al. 2015). Briefly, MRC-5 cells were plated in a 96-well plate at a density of 10^4 cells per well and incubated overnight in basal medium (Life Technologies) containing 10% fetal bovine serum (Hyclone), 1% L-glutamine (Life Technologies), 1% sodium bicarbonate (Life Technologies), 1% sodium pyruvate (Life Technologies), and 100 units/mL penicillin and 100 μg/mL streptomycin (Life Technologies), in a 37°C, 5% CO_2 incubator. Next day, serial dilutions of ABBV-615 were preincubated with IL-1β (human or cynomolgus monkey IL-1β at 200 pg/mL; rabbit IL-1β lysate generated from crude *E. coli* at 1:62500 dilution) for 1 h and then added to the cells with a final IL-1β concentration at approximately 3 pM. After an overnight incubation, supernatants were transferred to a 96-well round bottom plate and tested for human IL-8 using a Meso Scale Discovery human IL-8 assay kit according to manufacturer's instructions. The neutralization potency of ABBV-615 was determined by calculating average percent inhibition relative to the IL-1β alone control values. IC_{50} values were calculated by the GraphPad Prism 5 software (La Jolla, CA) using Four Parameter Logistic non-linear regression curve-fitting model.

Neutralization of rat and mouse IL-1β by ABBV-615 was measured in a CXCL1 release assay in a rat lung fibroblast cell line RLF-6 (ATCC). RLF-6 cells were determined to secrete rat CXCL1 in response to rat or mouse IL-1β stimulation. The RFL-6 bioassay was essentially the

same as MRC-5 bioassay except that the rat CXCL1 levels were measured by using a Meso Scale Discovery rat CXCL1 assay kit.

Neutralization of human and cynomolgus monkey IL-17A by ABBV-615 was measured in an IL-6 release assay in a human foreskin fibroblast cell line HS27 which secretes IL-6 in response to IL-17A. HS27 cells were cultured in DMEM high glucose medium (Life Technologies) containing 10% fetal bovine serum, 2 mM L-glutamine, 100 units/mL penicillin and 100 μg/mL streptomycin, and 1 mM sodium pyruvate . Serial dilutions of ABBV-615 were preincubated with human or cynomolgus monkey IL-17A and then added to HS27 cells plated in a 96-well plate at a density of 2×10^4 cells per well. The final concentration of each IL-17A was approximately 60 pM. After an overnight incubation, supernatants were collected and tested for human IL-6 by Meso Scale Discovery using a MSD human IL-6 assay kit. The neutralization potency of ABBV-615 was determined by calculating average percent inhibition relative to the IL-17A alone control values. IC_{50} values were calculated by the GraphPad Prism 5 software.

Neutralization of mouse, rat, and rabbit IL-17A by ABBV-615 was measured in a mouse embryo fibroblast cell line NIH3T3 (ATCC), which secretes IL-6 in response to IL-17A and TNF. The NIH3T3 bioassay was similar to the HS27 bioassay except that approximately 20-fold more NIH3T3 cells were incubated with ABBV-615/IL-17A preincubated mixture plus mouse TNF at a final concentration of 10 pM and IL-6 production was measured by using a Meso Scale Discovery mouse IL-6 assay kit.

JPET Fast Forward. Published on January 8, 2018 as DOI: 10.1124/jpet.117.243493
This article has not been copyedited and formatted. The final version may differ from this version.

Pharmacokinetics study in cynomolgus monkey

The *in vivo* studies with cynomolgus monkeys were carried out at AbbVie Inc., North Chicago, IL or MPI Research, Inc., 54943 North Main Street, Mattawan, Michigan 49071-8353MI in accordance with the Guide for the Care and Use of Laboratory Animals as adopted and promulgated by the U.S. National Institutes of Health, and were approved by the Institutional Animal Care and use Committee. Female cynomolgus monkeys (n=2/group) were administered ABBV-615 intravenously (i.v.) at 1 or 5 mg/kg (10 mg/mL in 30 mM histidine, 8% w/v sucrose, 0.02% polysorbate80, pH 6.0). Blood samples were collected from each monkey at 5 min, 4, 12 and 24 h, and 3, 7, 10, 14, 21 and 28 d post-dose. Serum samples were analyzed using with Meso Scale Discovery assay employing biotinylated human IL-1β for capture and Sulfo-Tag labeled human IL-17A for detection. Pharmacokinetic parameters for each animal were calculated with PLASMA rev 2.6.12 by non-compartmental analysis and linear trapezoidal method.

Dose range finding and tolerability study in cynomolgus monkey

Cynomolgus monkeys (1/sex/group) were administered dosages of 0, 20, or 100 mg/kg/dose of ABBV-615 at 0, 10, 50 mg/mL concentration, respectively in 15 mM histidine, 7.5 % sucrose, 0.016% Tween-80, pH 6.0 via i.v. injection once weekly for 6 weeks or 20 mg/kg/dose (at 20 mg/mL concentration) via subcutaneous (s.c.) injection once weekly for 6 weeks. Serial blood serum samples for an exposure-time profile of ABBV-615 were collected and analyzed from each animal on Day 1 (dose 1), and Day 36 (dose 6). Pre-dose 4 and 6 week blood samples were also collected and analyzed. Other parameters that were evaluated in the study included the following: mortality, clinical signs, body weight, hematology, coagulation and clinical chemistry. Dose proportionality was defined as proportional if mean C_{max} /Dose and $AUC_{0\text{-}168h}$

/Dose were within 0.5 to 2x of each other and the standard deviations overlap between dose groups in non-GLP and GLP cynomolgus monkey studies.

13-week cynomolgus monkey GLP toxicology study

ABBV-615 was administered i.v or s.c. once weekly for thirteen weeks (13 doses total) to cynomolgus monkeys (6/sex/group in control and 200 mg/kg/week IV and SC, respectively; 4/sex/group in low and mid dose groups) and reversibility or progression of any observed changes was assessed following a 12-week recovery period. The study details are summarized in Table 1. Dose proportionality was defined as proportional if mean C_{max} /Dose and $AUC_{0\text{-}168h}$ /Dose were within 0.5 to 2x of each other and the standard deviations overlap between dose groups in non-GLP and GLP cynomolgus monkey studies.

Assessment of toxicity was based on mortality, clinical observations, injection site observations, and body weight; ophthalmoscopic and electrocardiographic examinations; and clinical and anatomic pathology. Determination of ABBV-615 concentration and anti-drug antibody analysis was conducted on serum samples. Pre-dose and 15 min post dose plasma samples from study days 1 and 36 were analyzed for complement activation (i.e., CH50 increase with concomitant increase of the activation product C3a). Details are included in the supplementary information and Table S1. Blood neutrophil counts were specifically evaluated for changes using a two-way ANOVA with Bonferroni post-test.

In vitro human keratinocyte assays

Adult primary human keratinocytes from three healthy females were obtained from Thermo Fisher and maintained in Epilife Medium (Thermo Fisher) with Growth Supplements (Thermo Fisher). IL-17A was prepared by transiently overexpressing IL17A in HEK293 cells using

polyethylenimine (Sigma). Three days post transfection, supernatants were harvested and IL-17A was purified using standard immobilized metal affinity chromatography (IMAC) column (GE Healthcare, Little Chalfont, United Kingdom) chromatography. IL-17A was further purified using a Superdex 75 column (GE Healthcare). IL-1β was obtained from Sigma. To determine the keratinocyte response to IL-17A and IL-1β, cells were plated at a density of 10,000 cells/well in 96 well plates using Epilife medium with growth supplements except for the hydrocortisone. The next day, the media was exchanged and increasing concentrations of IL-17A and IL-1β were added. Culture supernatants were collected after 24 and 48 h. Concentrations of CXCL1 (R&D Systems, Minneapolis, MN), G-CSF (Meso Scale Discovery), LCN2 (R&D Systems), TNF (Meso Scale Discovery), IL-6 (Meso Scale Discovery), (Meso Scale Discovery), S100A8/9 (R&D Systems), and beta-defensin 2 (myBiosource, San Diego, CA) were determined using commercially available kits. The maximum fold inductions for each secreted factor were extrapolated from the data by dividing the maximum induction for each treatment group (i.e. IL-17A alone, IL-1β alone, or IL-17A/IL-1β combo) by background levels of the secreted factor.

JPET Fast Forward. Published on January 8, 2018 as DOI: 10.1124/jpet.117.243493
This article has not been copyedited and formatted. The final version may differ from this version.

6. Results

Combinatorial efficacy and inhibition of inflammatory mediators in mouse collagen-induced arthritis

In support of dual neutralization of IL-1β and IL-17A as a potential therapy for rheumatoid arthritis, we confirmed previously published studies in the collagen-induced arthritis (CIA) model in mice (Zhang, et al. 2013, Zwerina et al. 2012). While treatment with anti-IL-1β or anti-IL-17A mAb alone partially reduced paw swelling in the mouse CIA model, treatment with both antibodies significantly decreased paw swelling relative to the single antibody treatments (Figure 1A). In addition, histologic evaluation confirmed significantly greater inhibition of inflammation of the joint as well as prevention of cartilage damage and bone erosion with combination treatment compared to monotherapy (Figure 1B). Similar levels of serum anti-cytokine antibody levels were detected 96 h after the last dose in animals receiving either mono or combination therapy indicating that consistently high levels of treatment antibodies were present throughout the course of the study. Anti-IL-1β levels were 43$\pm$3 and 38$\pm$3 µg/mL in mono versus combination therapy and anti-IL-17A levels were 71$\pm$4 and 71$\pm$5 µg/mL, respectively. There were no treatment-related adverse events observed with single agent or combination antibody treatment, including weight loss, dehydration, hair loss, lethargy, or other health concerns(data not shown).

To define the molecular basis for the improved efficacy, microarray and protein analysis of paw homogenate from mice given single versus dual cytokine inhibition was performed. This analysis identified cytokines and chemokines, including IL-6, CXCL-1 and G-CSF, which

showed greater inhibition with the combination of both antibodies compared to single agent treatment (Table 2).

The combinatorial efficacy and inhibition of inflammatory meditators in mouse CIA prompted us to generate a dual specific antibody that simultaneously targets both human IL-1β and IL-17A and explore its feasibility for clinical evaluation in RA by testing in pharmacokinetics and toxicology studies in cynomolgus monkey.

Generation and characterization of anti-human IL-1β/IL-17A DVD-Ig ABBV-615

To generate a dual specific antibody that neutralizes both human IL-1β and IL-17A, a DVD-Ig molecule ABBV-615 was engineered from the variable domains of mAbs to human IL-1β and IL-17A (Figure 2A). The anti-IL-1β domain E26.35 in ABBV-615 is similar to the anti-IL-1β domain E26.13 in the anti-IL-1α/IL-1β DVD-Ig ABT-981 (Lacy et al., 2015); both share the same light chain and differ in only 4 amino acids in HC (one in CDR3 and 3 in frameworks 3). The anti-IL-17A domain in ABBV-615 was generated by PROfusion mRNA display technology. As determined by SPR analysis, ABBV-615 (generated from a CHO stable cell line) exhibited high affinity binding to human IL-1β (K_D = 11.6 ± 1.1 pM) and human IL-17A (K_D = 3.1 ± 0.9 pM), with fast on-rates at 10^5 ($M^{-1}s^{-1}$) range and slow off-rates at 10^{-6} (s^{-1}) range (Figure 2B). To determine if binding of one antigen to ABBV-615 interferes with binding of the other antigen under saturating conditions, the antigens were injected over captured ABBV-615 immediately one after another without any dissociation phase. Human IL-1β was able to bind captured ABBV-615 when human IL-17A was already bound (Figure 2C). Likewise, human IL-17A was able to bind captured ABBV-615 when human IL-1β was already bound. Based on the amount of the bound antigens and ABBV-615 capture levels, the

apparent stoichiometry for each antigen was determined to be 1.9 – 2.2. The stoichiometry data demonstrated that human IL-1β bound to both ABBV-615 binding domains even after both human IL-17A binding domains were saturated, and vice versa, implying that ABBV-615 was physically capable of simultaneously binding two human IL-1β molecules and two human IL-17A molecules.

The neutralization potency of ABBV-615 on human IL-1β and IL-17A was measured by analyzing cytokine production from MRC-5 and HS27 cells, respectively. Inhibition curves were generated by titrating increasing concentrations of ABBV-615 against hIL-1β (3 pM) or hIL-17A (60 pM), and the IC_{50} values were derived as described in the Methods. Consistent with the high affinity, ABBV-615 exhibited high neutralization potency on human IL-1β and human IL-17A, with IC_{50} at 3.3 ± 0.3 pM and 58.1 ± 4.7 pM, respectively (Figure 2D).

The species cross-reactivity of ABBV-615 was determined by potency assays and affinity measurement (Table 3). ABBV-615 (generated from HEK 293 cells) bound and neutralized cynomolgus monkey IL-1β and IL-17A with high affinity and potency, comparable to the human proteins. ABBV-615 neutralized rabbit IL-1β and IL-17A with moderate potencies with IC_{50} values at 1.4 ± 1.2 and 2.9 ± 1.8 nM, respectively, which are 50-130 fold reduced from the potencies on the human proteins. ABBV-615 exhibited poor binding and significantly reduced neutralizing activity on mouse and rat IL-1β and IL-17A (Table 3); thus, this agent could not be used in the murine CIA model of arthritis.

Pharmacokinetics with ABBV-615 in Cynomolgus Monkey

Because ABBV-615 is able to effectively neutralize both monkey IL-17A and IL-1β, with comparable potency to the human cytokines, cynomolgus is a pharmacologically relevant

animal species to conduct GLP toxicology studies. In initial pharmacokinetic studies in cynomolgus monkeys, ABBV-615 exhibited a bi-phasic concentration versus time profile with low clearance (mean CL = 0.065 mL/hr/kg) and low volume of distribution (mean V= 39.8 mL/kg) following a single intravenous dose of 1 and 5 mg/kg in cynomolgus monkey (Figure 3A, Table S2). Following 6 weekly doses in monkey, the C_{max} and $AUC_{0\text{-}168h}$ were approximately dose proportionally increased from 20 to 100 mg/kg i.v. doses (Figure 3B and C). ABBV-615 mean half-life in monkey was approximately 16 d and mean s.c. bioavailability was approximately 68% (Table S2). Lower exposure occurred following the sixth dose in one animal/group, probably due to the development of anti-drug antibodies (ADAs). Administration of six weekly dosages of ABBV-615 up to 100 mg/kg/dose by intravenous bolus, or 20 mg/kg/dose by s.c. injection was well tolerated in cynomolgus monkeys (one animal/sex/group). No adverse findings or any signs of toxicity were observed in this limited assessment (data not shown).

Toxicology of ABBV-615 in cynomolgus monkey

In order to examine longer term, repeat dose toxicology in a larger number of cynomolgus monkeys, ABBV-615 was administrated by s.c. injection at 20, 65, and 200 mg/kg/week or by i.v. bolus injection at 200 mg/kg/week for 13 weeks Table 4. From 20 to 200 mg/kg/week s.c. dose levels, C_{max} and $AUC_{0\text{-}168h}$ were increased approximately dose proportionally (Supplemental Table S2). Five of 40 animals dosed with ABBV-615 (one each at 20 and 65 mg/kg/week, two at 200 SC and one at 200 IV) showed a confirmed anti-ABBV-615 antibody titer (ADA) (supplemental information). In this study, administration of ABBV-615 resulted in three unscheduled deaths, one male at 65 mg/kg/week with s.c. dosing,one female at 200 mg/kg/week with i.v. dosing and another female at 200 mg/kg/week with i.v. dosing because of

a broken humerus (Table 4). The death/moribundity of the first two animals was due to generalized infection/septicemia and were considered to be indirectly related to ABBV-615 but adverse (supplemental information). Both animals exhibited clinical signs of declining health status such as decreased activity/lethargy, hunched posture, dehydration, and/or impaired hind limb function. In addition they showed changes in clinical pathology parameters that were secondary to inflammation including a decrease in red cell mass, increase in fibrinogen and globulin, as well as reduced food intake and/or general ill health such as decreases in sodium, chloride, phosphorus, and total protein (Table S4)). At the terminal necropsy, ABBV-615-related generalized infection/septicemia was also present in one 65 mg/kg/week male with s.c. dosing, and as with the unscheduled death animals was deemed adverse (Table 4 and supplemental information). ABBV-615-related clinical signs for surviving animals included nodules at 200 mg/kg/week with s.c. dosing and 200 mg/kg/week with i.v. dosing and abscesses at 20 and 65 mg/kg/week with s.c. dosing and 200 mg/kg /week with i.v. dosing (Table 4 and supplemental information) which correlated to secondary decreases in red cell mass (Table S3A and B). There were increases in globulin and/or fibrinogen and/or decreases in albumin, albumin/globulin ratio that were evidence of an inflammatory response at 200 mg/kg/week with s.c. or i.v. dosing. While increased skin infections can be associated with neutropenia (Gonzalez-Barca, et al. 2001), there were no consistent neutrophil changes over dose or time (Figure 4), and other hematological parameters remained unchanged (Table S3A and B). Complement activation analysis did not show any evidence for complement activation by measuring total classical pathway activity (CH50 assay) and level of the activation product C3a in pre-dose and 15 min post dose samples from study days 1 and 36 (Table S1). Furthermore, there were also no notable histopathological changes to the skin outside of the

abscesses or injection sites. Changes in clinical pathology parameters were generally reversible following the 12-week recovery period (data not shown). At the terminal necropsy, ABBV-615-related non-adverse mononuclear cell infiltration consisting of focal infiltrates of macrophages and lymphocytes was present in subcutaneous injection sites from males at ≥65 mg/kg/week with s.c. dosing and females at ≥20 mg/kg/week with s.c. dosing (supplemental information).

In contrast to the observations with ABBV-615, data generated in separate experiments with agents that neutralize only IL-17A (anti-IL-17A mAb) or IL-1 [anti-IL-1α/anti-IL-1β DVD-Ig molecule (Lacy, et al. 2015)] showed no evidence for skin abscesses or increased sensitivity towards septicemia in 13-week repeat-dose toxicology studies in cynomolgus monkeys using identical high dose levels of 200 mg/kg/week with i.v. and s.c. dosing (for more details see table 5). As the affinities, potencies and *in vivo* exposure levels of the anti-IL-17A and IL-1α/β DVD-Ig were similar to treatment with ABBV-615 (Table 5), these results clearly demonstrate that neutralization of both IL-17A and IL-1β is needed to increase the sensitivity for skin infections in cynomolgus monkey.

Production of anti-microbial factors by human epidermal keratinocytes

In an effort to understand the mechanisms contributing to increased susceptibility to skin infections with dual neutralization of IL-1β and IL-17A, we explored the effects of IL-1β and IL-17A co-stimulation on cytokine, chemokine, and anti-microbial peptide secretion from normal human epidermal keratinocytes *in vitro*. IL-1β, IL-17A, or combination treatment significantly increased the production of IL-6, TNF, LCN2, CXCL1, G-CSF and IL-8 (Figure 5). We also evaluated β-defensin 2 and S100A8/9 levels in these cultures, however, β-defensin

2 was not upregulated by either IL-17A or IL-1β (data not shown), and increases in S100A8/9 did not consistently reach statistical significance (data not shown).

IL-1β treatment had the strongest effect on IL-6 and TNF producing 8 fold increases over untreated control. In contrast, IL-17A strongly increased LCN2 and G-CSF (9-11 fold). Lastly, IL-8, CXCL1 and G-CSF demonstrated greater induction with co-stimulation relative to single IL-1β or IL-17A alone. G-CSF in particular was highly sensitive to co-stimulation with a 162 fold increase over untreated control, while showing only 6 and 11 fold increases with IL-1β or IL-17A alone, respectively. Thus, the single agent and combinatorial treatments with IL-17A and IL-1β showed different patterns of induction for key cytokines, chemokines and anti-microbial factors that are important for defense against skin infections.

7. Discussion

As a strategy to improve efficacy in rheumatoid arthritis and potentially other inflammatory diseases, we utilized dual-variable domain (DVD-Ig) technology to simultaneously target both IL-1β and IL-17A. Similar to other previously reported results (Zwerina, et al. 2012, Wu, et al., 2016, Zhang et al., 2013), depletion or blockade of both IL-1β and IL-17A improved efficacy in a mouse model of arthritis over individual agents, supporting the potential combinatorial effects for treatment of disease. A dual variable domain antibody, ABBV-615 was generated that neutralizes human and cynomolgus monkey IL-1β and IL-17A with high potency, binding both cytokines simultaneously and shows antibody-like pharmacokinetics in cynomolgus monkeys. In a 13-week repeat-dose cynomolgus monkey toxicology study ABBV-615 demonstrated an increased incidence of skin infections in a time-dependent manner at all doses tested, while historic data with either anti-IL-17A or anti-IL-1α/β DVD-Ig neutralizing antibodies did not demonstrate any evidence of increased infections in monkeys at similar exposure levels and similar treatment duration. The increase in infections was not attributable to decreases in circulating neutrophils or changes in other hematological parameters. These results provide evidence in non-human primates that the presence of either IL-1β or IL-17A is required specifically for defense against skin infections.

While preclinical and clinical studies with single agent IL-1 or IL-17A neutralization show minimal safety risk, there is evidence that these two cytokines are each important in defense against skin infections (Miller and Cho, 2011). IL-17A is important in defense against *Candida albicans* as patients with mutations in IL-17A or IL-17 receptor show susceptibility to chronic candidiasis as well as *Staphylococcus (S.) aureus* (Puel, et al., 2011; McDonald, 2012).

IL-17 receptor knock out (KO), IL-1β or IL-1R KO mice show reduced dermal *S. aureus* bacterial clearance and increased abscess size and reduced neutrophil recruitment (Miller, et al., 2007, Cho, et al., 2010, Cho et al., 2011; Maher, et al. 2013). In addition, IL-1β and IL-17A are both able to induce a variety of anti-microbial and neutrophil chemotactic factors in human keratinocytes or cell lines, including β-defensins, cathelicidin, S100 calcium binding proteins (S100)A8 andA9, CXCL1, CXCL5 and IL-8, which have been shown to contribute to anti-bacterial defense (Krishna and Miller, 2012; Olaru and Jensen, 2010).

The emergence of skin infections in cynomolgus monkeys following dual blockade with IL-1β and IL-17A supports that these cytokines play a redundant role in the protection from skin infection. Anakinra, a recombinant form of IL-1 receptor antagonist, had a similar safety profile to placebo, with the exception of injection-site reactions, in a clinical trial in methotrexate- inadequate responder RA patients (Cohen, et al., 2004). AMG 108, an antibody targeting IL-1 receptor, showed a similar lack of adverse events in a rheumatoid arthritis trial (Cardiel, et al., 2010). Furthermore, canakinumab, a human anti-IL-1β mAb in rheumatoid arthritis patients showed comparable adverse events compared to placebo with no increase in infections (Alten, et al., 2011). Finally, the anti-IL-17A monoclonal antibody, secukinumab, in rheumatoid arthritis also demonstrated a comparable safety profile to other biologics, with no dose-dependent effects on the incidence of adverse events. There was a slightly higher incidence of upper respiratory infections, but no noted skin infections (Genovese, et al., 2013). Thus, in contrast to dual neutralization, single IL-1 or IL-17A neutralizing agents showed little evidence of increasing cutaneous infectious risk in either monkeys or humans.

JPET Fast Forward. Published on January 8, 2018 as DOI: 10.1124/jpet.117.243493
This article has not been copyedited and formatted. The final version may differ from this version.

While we did not definitively identify the nature of the bacterial infection seen in cynomolgus monkeys treated with ABBV-615, neutrophilic abscesses are a hallmark of *S. aureus* infections in addition to the reported roles of IL-1 and IL-17A in defense against this infection. Additionally, we did observe gram positive cocci in one of the animals exhibiting an abscess. Immune activation in the skin by *S. aureus* appears to be through toll-like receptor 2 activation, which induces IL-1β, IL-6 and IL-23 (Miller and Cho, 2011; Krishna and Miller, 2012). IL-1β and IL-23 induce IL-17A production from natural killer T cells, Th17 cells, α/β T cells and natural killer cells (Cua and Tato, 2010) and can do so in the absence of T cell receptor engagement (Dungan and Mills, 2011). The IL-17A and IL-1β also induce keratinocytes to produce chemokines (CXCL1, CXCL2, IL-8) to recruit neutrophils and anti-microbial peptides/proteins (beta-defensins, cathelicidin, lipocalin 2) which have bacteriocidal or bacteriostatic activities (Ryu, et al., 2014; Olaru and Jensen, 2010; Dungan and Mills, 2011). IL-1β also appears to limit the production of the immune suppressive cytokine, IL-10, by Th17 cells that are specific for *S. aureus* (Zielinski, et al., 2012). Amplification of the recruitment can occur through IL-1β and IL-17A-induced anti-microbial proteins and chemokines, such as CCL20, which recruit additional immune cells, including Th17 cells (Miller and Cho, 2011; Ryu, et al., 2014). All these activities highlight the cooperative role of IL-1β and IL-17A in defense against skin infections that was confirmed in the present studies.

The skin restricted susceptibility to infection with dual IL-1β and IL-17A neutralization suggests a central role for skin resident stromal and/or parenchymal cells such as keratinocytes, propagating the induction of neutrophil-attracting chemokines and anti-microbial proteins in response to IL-17A and IL-1β (Miller and Cho, 2011). Our *in vitro* results suggest that both IL-17A and IL-1β have a unique keratinocyte signature with certain secreted factors showing

more IL-17A sensitivity (LCN2), others showing more IL-1β sensitivity (TNF and IL-6), and still others (IL-8, CXCL1, and G-CSF) being most sensitive to co-stimulation with IL-17A and IL-1β. These differences in the keratinocyte secretome highlight the increased impact of neutralizing two different cytokines.

This apparent overlap between the immune response and the keratinocyte response, as well as a potential model for the infection susceptibility with ABBV-615, is summarized in Figure 6. In this model of skin infection, invading bacteria initiate an IL-1β producing myeloid response and an IL-17A producing lymphocyte response in parallel to resolution of the infection. Both of these parallel pathways converge at skin resident stromal and parenchymal cells, which directly help fight off the infection with bactericidal peptides/proteins (e.g. LCN2) and also amplify the immune response by producing cytokines and chemokines (e.g. IL8, IL-6, TNF, CXCL1). In this model, each stimulus can access some unique outputs from keratinocytes as well as some shared outputs. Inhibiting only IL-17A or IL-1β may leave enough of the keratinocyte response intact to prevent infection but neutralizing both IL-1β and IL-17A simply reduces too many key chemokines and anti-microbial peptides.

The induction of G-CSF, CXCL1, and IL-6 production by IL-17A and/or IL-1β proteins in keratinocytes were consistent with the inhibition of these factors at the gene and protein levels in paw homogenates from the mouse arthritis model following treatment with anti-IL-17A and anti-IL-1β. Thus, while playing a key role in a disease setting (arthritis), IL-1β and IL-17A also appear to play a protective role specifically in skin infections and reinforce the hypothesis that dual inhibition of IL-1β and IL-17A has a much broader impact than single cytokine inhibition.

JPET Fast Forward. Published on January 8, 2018 as DOI: 10.1124/jpet.117.243493
This article has not been copyedited and formatted. The final version may differ from this version.

Increased infection risk has been observed clinically in short term studies with other combinations of approved therapies tested in RA, including anakinra (IL-1R antagonist) plus etanercept (soluble TNF receptor that blocks TNF) as well as abatacept (blocking co-stimulation of T-cells) plus anti-TNF (Genovese, et al., 2004; Weinblatt, et al., 2006; Weinblatt, et al., 2007). A few patients developed cellulitis, and there were also cases of respiratory, gastrointestinal, ear or urinary infections as well as herpes, candidiasis and pneumonia infections (Genovese, et al., 2004, Weinblatt, et al., 2006, Weinblatt, et al., 2007). Neither of these combinations noted an increase in abscessing cutaneous infections as we saw in the cynomolgus monkey study with ABBV-615. Thus, the specificity to abscessing skin infections may be unique to the dual neutralization of IL-1β and IL-17A, although this would have to be verified in a human clinical study. Importantly, these results of dual inhibition are likely not related to the nature of the bispecific molecule used in this study but would likely have been found in any other dual specific format or even with separate dosing of two antibodies. Therefore caution should be exercised in combining anti-IL-1 and anti-IL-17A biologic agents in patients.

In summary, the increase in skin infections in monkeys upon dual neutralization of IL-1 and IL-17A with ABBV-615 demonstrated the importance of leaving either IL-1β or IL-17A pathways intact in a system relevant to humans. While cytokines often show redundant activities, this particular combination blockade for IL-1β and IL-17A revealed a specific role of these two cytokines in cutaneous infections and highlights the need to better understand immune interactions.

8. Acknowledgements

The authors wish to thank Carrie Goodreau, Maria Harris, Jijie Gu, and Tariq Ghayur for the generation of ABBV-615, and Renee Miller, Alyssa Brito, Sahana Bose, Georgeen Gaza-Bulseco, Michele Diloreto, and Margaret Hugunin for contributions to *in vitro* characterization of ABBV-615. We also acknowledge the Abbvie Research Center's Animal facilities at Abbvie Research Center and Lake County sites for mouse and cynomolgus monkey pharmacokinetics and tolerability studies as well as MPI contract research organization for their assistance with the GLP cynomolgus monkey toxicity study.

9. Authorship contributions

Participated in research design: Ruzek, Huang, Zhang, Bryant, Slivka, Cuff, Tripp and Blaich

Conducted experiments: Bryant, Slivka

Performed data analysis: Ruzek, Huang, Zhang, Bryant, Slivka, and Blaich

Wrote or contributed to the writing of the manuscript: Ruzek, Huang, Zhang, Bryant, Slivka, Cuff, Tripp and Blaich

10. References

Alten R, Gomez-Reino J, Durez P, Beaulieu A, Sebba A, Krammer G, Preiss R, Arulmani U, Widmer A, Gitton X, Kellner H (2011) Efficacy and safety of the human anti-IL-1beta monocloncal antibody canakinumab in rheumatoid arthritis: results of a 12-week, phase II, dose-finding study. BMC Musculoskeletal Disorders 12:153.

Canavan TN, Elmets CA, Cantrell WL, Evans JM, Elewski BE (2016) Anti-IL-17 medications used in the treatment of plaque psoriasis and psoriatic arthritis: a comprehensive review. Am J Clin Dermatol 17:33-47.

Cardiel MH, Tak PP, Bensen W, Burch FX, Forejtova S, Badurski JE, Kakkar T, Bevirt T, Ni L, McCroskery E, Jahreis A, Zach DJ (2010) A phase 2 randomized, double blind study of AMG108, a fully human monoclonal antibody to IL-1R, in patients with rheumatoid arthritis. Arthritis Res Ther 12: R192.

Cho JS, Pietras EM, Garcia NC, Ramos RI, Farzam DM, Monroe HR, Magorien JE, Blauvelt A, Kolls JK, Cheung AL, Cheng G, Modlin RL, Miller LS (2010) IL-17 is essential for host defense against cutaneous *Staphylococcus aureus* infection in mice. J Clin Invest 120: 1762-1773.

Cho JS, Zussman J, Donegan NP, Ramos RI, Garcia NC, Uslan DZ, Iwakura Y, Simon SI, Cheung AL, Modlin RL, Kim J, Miller LS (2011) Noninvasive in vivo imaging to evaluate immune responses and antimicrobial therapy against *Staphylococcus aureus* and USA300 MRSA skin infections. J Invest Dermatol 131:907-915.

Choy E (2012) Understanding the dynamics: pathways involved in the pathogenesis of rheumatoid arthritis. Rheumatology 51:v3-v11.

Cohen SB, Moreland LW, Cush JJ, Greenwald MW, Block S, Shergy WJ, Hanrahan PS, Khraishi MM, Patel A, Sun G, Bear MB (2004) A multicenter, double blind, randomized, placebo controlled trial of anakinra (Kineret), a recombinant interleukin 1 receptor antagonist, in patients with rheumatoid arthritis treated with background methotrexate. Ann Rheum Dis 63:1062-1068.

Cua DJ, Tato CM (2010) Innate IL-17-producing cells: the sentinels of the immune system. Nat Rev Immunol 10: 479-489.

Dungan LS, Mills KHG (2011) Caspase-1-processed IL-1 family cytokines play a vital role in driving innate IL-17. Cytokine 56:126-132.

Genovese MC, Durez P, Richards HB, Supronik J, Dokoupilova E, Mazurov V, Aelion JA, Lee S-H, Codding CE, Kellner H, Ikawa T, Hugot S, Mpofu S (2013) Efficacy and safety of secukinumab in patients with rheumatoid arthritis: a phase II, dose-finding, double-blind, randomized, placebo controlled study. Ann Rheum Dis 72: 863-869.

Genovese MC, Cohen S, Moreland L, Lium D, Robbins S, Newmark R, Bekker P (2004) Combination therapy with etanercept and anakinra in the treatment of patients with rheumatoid arthritis who have been treated unsuccessfully with methotrexate. Arthritis Rheum 50: 1412-1419.

González-Barca E, Carratalà J, Mykietiuk A, Fernández-Sevilla A, Gudiol F (2001) Predisposing factors and outcome of Staphylococcus aureus bacteremia in neutropenic patients with cancer. Eur J Clin Microbiol Infect Dis 20:117-119.

Jesus AA, Goldbach-Mansky R (2014) IL-1 blockade in autoinflammatory syndromes. Annu Rev Med 65:223-244.

Krishna S, Miller LS (2012) Innate and adaptive immune responses against *Staphylococcus aureus* skin infections. Semin Immunopathol 34:261-280.

Lacy SE, Wu C, Ambrosi DJ, Hsieh C-M, Bose S, Miller R, Conlon DM, Tarcsa E, Chari R, Ghayur T, Kamath RV (2015) Generation and characterization of ABT-981, a Dual Variable Domain Immunoglobulin (DVD-Ig™) molecule that specifically and potently neutralizes both IL-1α and IL-1β. mAbs 7: 605-619.

Maher BM, Mulcahy ME, Murphy AG Wilk M, O'Keefe KM, Geoghegan JA, Lavelle EC, McLoughlin RM (2013) Nlrp-3-driven interleukin-17 production by γδT cells controls infection outcomes during *Staphylococcus aureus* surgical site infection. Infect Immun 81: 4478-4489.

Mateen S, Zafar A, Moin S, Khan AQ, Zubair S (2016) Understanding the role of cytokines in the pathogenesis of rheumatoid arthritis. Clin Chim Acta 455: 161-171.

McDonald DR (2012) T_H17 deficiency in human disease. J Allergy Clin Immunol 129:1429-1435.

Miller LS, Cho JS (2011) Immunity against *Staphylococcus aureus* cutaneous infections. Nat Rev Immunol 11: 505-518.

Miller LS, Pietras EM, Uricchio LH, Hirano K, Rao S, Lin H, O'Connell RM, Iwakura Y, Cheung AL, Cheng G, Modlin RL (2007) Inflammasome-mediated production of IL-1β is required for neutrophil recruitment against *Staphylococcus aureus* in vivo. J Immunol 179:6933-6942.

Olaru F, Jensen LE (2010) Staphylococcus aureus stimulates neutrophil targeting chemokine expression in keratinocytes through an autocrine IL-1α signaling loop. J Invest Dermatol 130:1866-1876.

Puel A, Cypowyj S, Bustamante J, Wright JF, Liu L, Lim HK, Miguad M, Israel L, Chrabieh M, Audry M, Gumbleton M, Toulon A, Bodemer C, El-Baghdadi J, Whitters M, Paradis T, Brooks J, Collins M, Wolfman NM, Al-Muhsen S, Galicchio M, Abel L, Picard C, Casanova J-L (2011) Chronic mucocutaneous candidiasis in humans with inborn errors of interleukin-17 immunity. Science. 332: 65-68.

Ryu S, Song PI, Seo CH, Cheong H, Park Y (2014) Colonization and infection of the skin by *S. aureus*: Immune system evasion and the response to cationic antimicrobial peptides. Int J Mol Sci 15:8753-8772.

Weinblatt M, Schiff M, Goldman A, Kremer J, Luggen M, Li T, Chen D, Becker J-C (2007) Selective costimulation modulation using abatacept in patients with active rheumatoid arthritis while receiving etanercept: a randomized clinical trial. Ann Rheum Dis 66: 228-234.

Weinblatt M, Combe B, Covucci A, Aranda R, Becker JC, Keystone E (2006) Safety of the selective costimulation modulatory abatacept in rheumatoid arthritis patients receiving background biologic and nonbiologic disease-modifying antirheumatic drugs. Arthritis Rheum 54:2807-2816.

Wu C, Ying H, Grinnell C, Bryant S, Miller R, Clabbers A, Bose S, McCarthy D, Zhu RR, Santora L, Davis-Taber R, Kunes Y, Fung E, Schwartz A, Sakorafas P, Gu J, Tarcsa E, Murtaza A, Ghayur T (2007) Simultaneous targeting of multiple disease mediators by a dual-variable-domain immunoglobulin. Nat Biotechnol 25:1290-1297.

Wu Q, Wang Y, Wang Q, Yu D, Wang Y, Song L, Liu Z, Ye X, Xu P, Cao H, Li D, Ren G (2016) The bispecific antibody aimed at the vicious circle of IL-1β and IL-17, is beneficial for the collagen-induced rheumatoid arthritis of mice through NF-kB signaling pathway. Immunology Letters 179:68-79.

Zhang Y, Ren G, Guo M, Ye X, Zhao J, Xu L, Qi J, Kan F, Liu M, Li D (2013) Synergistic effects of interleukin-1β and interleukin-17A antibodies on collagen-induced arthritis mouse model. Int Immunopharmacol 15: 199-205.

Zielinski CE, Mele F, Aschenbrenner D, Jarrossay, Ronchi F, Gattorno M, Monticelli S, Lanzavecchia A, Sallusto F (2012) Pathogen-induced human T_H17 cells produce IFN-γ or IL-10 and are regulated by IL-1β. Nature 484: 514-518.

Zwerina K, Koenders M, Hueber A, Marijnissen RJ, Baum W, Heiland GR, Zaiss M, McInnes I, Joosten L, van den Berg W, Zwerina J, Schett G (2012) Anti-IL-17 therapy inhibits bone loss in TNF-α-mediated murine arthritis by modulation of the T-cell balance. Eur J Immunol 42:413-423.

11. Footnotes

†The design, study conduct, and financial support for the study were provided by Abbvie. Abbvie participated in the interpretation of data, review and approval of the publication work was funded by Abbvie, Inc.

MR, LH, TTZ, SB, PFS, CAC, and GB are employees of Abbvie. CT was an employee of Abbvie at the time of the study.

*Corresponding author

Reprint requests sent to:

Melanie Ruzek

Abbvie Bioresearch Center

100 Research Drive

Worcester, MA 01605

Melanie.ruzek@abbvie.com

12. Legends for Figures

Figure 1. Combination treatment with anti-IL-1ß and anti-IL-17A is superior to monotherapy in a therapeutic model of mouse CIA. (A) Paw (footpad) thickness of CIA mice was measured daily by caliper. Baseline was subtracted for each individual mouse before the onset of disease. Data is expressed as change in paw thickness (mm). (B) Histopathology was performed on rear paws and visually scored from 0-4 based on the severity of inflammation, cartilage damage, and bone destruction. $*P < 0.05$ versus vehicle; $\wedge P < 0.05$ versus monotherapy ($n = 12$). Data are expressed as the mean ± S.E. and is a representative of 3 experiments.

Figure 2. Construction and characterization of anti-IL-1β/IL-17A DVD-Ig ABBV-615. (**A**) Schematic diagram of ABBV-615 DVD-Ig with the anti-IL-1β variable domain in the outer position linked to the anti-IL-17A variable domain in the inner position. (**B**) Affinity measurement of ABBV-615 by SPR. Dissociation was monitored for 1500 s for hIL-1β binding. Due to the very slow off-rates for hIL-17A binding, dissociation was monitored for 3900 s for high hIL-17A concentration (50 and 100 nM) and for 850 s for lower concentrations (1.56 – 25 nM). The affinity (K_D) (mean ± S.D.) based on 3 independent experiments is 11.6 ± 1.1 pM for hIL-1β binding and 3.1 ± 0.9 pM for IL-17A binding. Representative sensorgrams are shown. (**C**) Sequential binding of human IL-17A and IL-1β to ABBV-615 by SPR. Left: hIL-17A was injected first followed immediately by injection of hIL-1β. Right: hIL-1β was injected first followed immediately by injection of hIL-17A. Representative sensorgrams with sequential injections of antigens are shown. (**D**) ABBV-615 potency by cell-based bioassay. Neutralization potency of ABBV-615 on hIL-1β and hIL-17A was determined by IL-8 release

assay in MRC-5 cells and IL-6 release assay in HS27 cells, respectively. ABBV-615 neutralization potency (IC_{50}) (mean ± S.E.) on hIL-1β and hIL-17A calculated from 3 independent experiments is 3.3 ± 0.3 pM and 58.1 ± 4.7 pM, respectively. Representative inhibition data are shown. Plotted in Y-axis is % inhibition relative to the hIL-1β or hIL-17A alone control.

Figure 3: Single and repeat dosing of ABBV-615 in cynomolgus monkeys demonstrates acceptable pharmacokinetic properties. (A). Individual ABBV-615 serum concentration versus time profile following single intravenous dose of 1 mg/kg and 5 mg/kg (2 female/group). (B). Individual ABBV-615 serum concentration versus time profile following six weekly intravenous doses of 20 mg/kg and 100 mg/kg and subcutaneous dose of 20 mg/kg after Dose 1. (C). Individual ABBV-615 serum concentration versus time profile following six week weekly intravenous doses of 20 mg/kg and 100 mg/kg and subcutaneous dose of 20 mg/kg after Dose 6 (1 female + 1male /group).

Figure 4. Neutrophil counts (mean ± S.E.) from monkeys (males and females combined) over the course of the 13-week toxicology study with ABBV-615 (group 1 = control s.c./i.v., groups 2-4 = 20, 65 and 200 mg/kg/week s.c. and group 5 = 200 mg/kg/week i.v.; 6 animals/sex in groups 1, 4 and 5; 4 animals/sex in groups 2 and 3).

Figure 5. Primary human epidermal keratinocyte production of anti-bacterial factors upon treatment with IL-1β and IL-17A. Secreted levels of IL-6, TNF, LCN2, G-CSF, CXCL1 and IL-8 in response to titrations of IL-17A (200-0.2 ng/mL) and IL-1β (50-0.2 ng/mL) at 48 h post

stimulation are shown. Three different induction patterns are illustrated: (A, B) IL-1β-driven, (C) IL-17A-driven, and (D-F) co-stimulation-driven. The maximum fold induction versus untreated control for each secreted factor after treatment with IL-17A, IL-1β, or IL-17A/IL-1β co-stimulation (G) is also shown. A total of three individual human keratinocyte donors were tested (one experiment per donor). Data is expressed as mean ± S.E. from one of three representative donors.

Figure 6. Illustration of combinatorial IL-1β and IL-17A activities contributing to bacterial clearance in the skin (A) and proposed how ABBV-615 increases skin infection susceptibility by blockade of both IL-1β and IL-17A (B)(modified from Ryu, et al. 2014, *Colonization and infection of the skin by S. aureus: Immune system evasion and the response to cationic antimicrobial peptides.* http://www.mdpi.com/1422-0067/15/5/8753 Copyright © 2014 by the authors; licensee MDPI, Basel, Switzerland. This image is open access distributed under the terms and conditions of the Creative Commons Attribution license, http://creativecommons.org/licenses/by/3.0/).

JPET Fast Forward. Published on January 8, 2018 as DOI: 10.1124/jpet.117.243493
This article has not been copyedited and formatted. The final version may differ from this version.

13. Tables

TABLE 1

Study design for 13-week cynomolgus monkey toxicology study

Dose level (mg/kg/week)	Dose Volume (mL/kg/week)	Dose Concentration (mg/mL)	Number of Males	Number of Females
0/0 (i.v./s.c.)	2/2[a]	0/0	6[b]	6[b]
20 s.c.	2	10	4	4
65 s.c.	2	32.5	4	4
200 s.c.	2	100	6[b]	6[b]
200 i.v.	2	100	6[b]	6[b]

[a]Animals received vehicle (15 mM histidine, 75 mg/mL sucrose, 0.0163% Tween 80, pH 6.0) both i.v. and s.c., about 5 min apart.

[b]Two animals/sex/group were maintained for a 12-week recovery period.

JPET Fast Forward. Published on January 8, 2018 as DOI: 10.1124/jpet.117.243493
This article has not been copyedited and formatted. The final version may differ from this version.

TABLE 2

Dual neutralization of IL-1β and IL-17A cooperatively inhibits CXCL1, IL-6 and G-CSF gene and protein expression in paw homogenate from mouse CIA model

Cytokine/ chemokine	Paw homogenate gene expression inhibition relative to untreated [a]			Paw homogenate protein inhibition relative to untreated [a]		
	Anti-IL-1β	Anti-IL-17A	Combination	Anti-IL-1β	Anti-IL-17A	Combination
G-CSF	None	None	19 ± 4	30 ± 32	23 ± 5	92 ± 4[b]
IL-6	34 ± 27	33 ± 16	87 ± 4[b]	2 ± 28	13 ± 17	72 ± 12[b]
KC (CXCL1)	47 ± 10	33 ± 6	73 ± 7[b]	11± 18	8 ± 39	66 ± 14

[a] data shown are mean % change ± S.E. from 4 or 5 animals per group for gene and protein inhibition, respectively.

[b] $p<0.05$

JPET Fast Forward. Published on January 8, 2018 as DOI: 10.1124/jpet.117.243493
This article has not been copyedited and formatted. The final version may differ from this version.

TABLE 3

Species cross-reactivity of ABBV-615

Species	IL-1β cross-reactivity[a]		IL-17A cross-reactivity[a]	
	Potency (IC_{50}, pM)	Affinity (K_D, pM)	Potency (IC_{50}, pM)	Affinity (K_D, pM)
Human	11 ± 6	6.2 ± 2.1	60 ± 9	≤ 2
Cynomolgus	7 ± 3	2.6 ± 1.4	163 ± 24	≤ 8.3
Mouse	11233 ± 7105	10800 ± 809	> 50000	Low binding[b]
Rat	>50000	Low binding[b]	12000 ± 3237	Low binding[b]
Rabbit	1422 ± 685	ND[c]	2900 ± 1000	400 ± 98

[a]data shown are mean ± S.E. from 3 independent experiments

[b]poor binding response with very low signal measured in the SPR (BIAcore) assay

[c]not determined due to the lack of purified rabbit IL-1β protein

JPET Fast Forward. Published on January 8, 2018 as DOI: 10.1124/jpet.117.243493
This article has not been copyedited and formatted. The final version may differ from this version.

TABLE 4

Overview on incidence of infections and time of onset, skin abscesses and moribundity

Dose Group (mg/kg/week, route)	Study Week	Abscesses: incidence per dose group[c]	Findings and Location
20, s.c.	13	1/8	Abscess, corner of mouth
65, s.c.	6	1/8	Abscess at lower lip and under chin[a] Euthanized because of septicemia/inflammation (Day 38)[a,b]
65, s.c.	8 12	2/8	Nodule/abscess on dorsal surface[a] Abscess, left and right foot[a]
65, s.c.	13	3/8	Abscess, dorsal surface
200, i.v.	4	1/12	Abscess at base of tail Euthanized in extremis with broken humerus (Day 51)
200, i.v.	7	2/12	Left inguinal nodule/abscess
200, i.v.	7	3/12	Swelling on back of knee/abscess right hind limb
200, i.v.	8	4/12	Abscess on left and right forelimb
200, i.v.	11	N/A	Euthanized because of septicemia/inflammation (Day 74); animal did not show clinically an abscess[a]
200, i.v.	12	5/12	Abscess, left hind limb

[a]microscopy showed inflammation and septicemia in various organs (heart, lung, muscle, etc) in these animals

[b]moribund monkey; gram positive cocci bacterial colonies were observed in the heart and subcutis using Brown-Brenn Gram staining.

[c]study design: 6 animals/group/sex in control, 200 i.v. and 200 s.c.; 4 animals/group/sex at 20 and 65 s.c.

JPET Fast Forward. Published on January 8, 2018 as DOI: 10.1124/jpet.117.243493
This article has not been copyedited and formatted. The final version may differ from this version.

TABLE 5

ABBV-615, IL-17A-mAb and IL-1α/IL-1β DVD-Ig: A comparison of (a) exposure data after dosing for 13 weeks at 200 mg/kg/week i.v. or s.c. in cynomolgus monkey, (b) potency and affinity regarding IL-17A and IL-1β, (c) total incidence of skin abscesses at top doses of 200 mg/kg/week, and (d) total incidence of skin abscesses at all dose levels tested

Compound	200 mg/kg/week i.v.		200 mg/kg/week s.c.		Affinity		Potency (IC_{50})		Overall incidence skin abscesses at 200 mg/kg i.v. and s.c.	Overall incidence skin abscesses at all dose levels tested
	C_{max}	AUC	C_{max}	AUC	IL-17A	IL-1β	IL-17A	IL-1β		
Anti-IL-17A mAb[a]	9.44	792	4.39	569	0.8	---	9	---	0/16	0/32
Anti-IL 1α / IL-1β DVD-Ig[b]	10.9	723	2.90	369	---	28	---	26	0/20	0/40
ABBV-615	11.9	1160	4.95	720	3	12	58	3	5/24	9/40

[a] Study design of 13-week study: Control (i.v./s.c.), 20, 60 and 200 (all i.v.) and 200 s.c.; 4 animals/group/sex (= a total of 32 animals dosed with anti-IL-17A mAb)

[b] Study design of 13-week study: Control (i.v./s.c.), 50, 100 and 200 (all i.v.) and 200 s.c.; 6 animals/group/sex in control, 50 and 200 i.v., 4 animals at 100 mg i.v. and 200 s.c. (= a total of 40 animals dosed with the DVD-Ig)

Unit: C_{max} is mg/mL; AUC is $AUC_{0\text{-}168h}$ at mg·h/ mL; Affinity and Potency IC_{50} are pM

JPET Fast Forward. Published on January 8, 2018 as DOI: 10.1124/jpet.117.243493
This article has not been copyedited and formatted. The final version may differ from this version.

Figure 1.

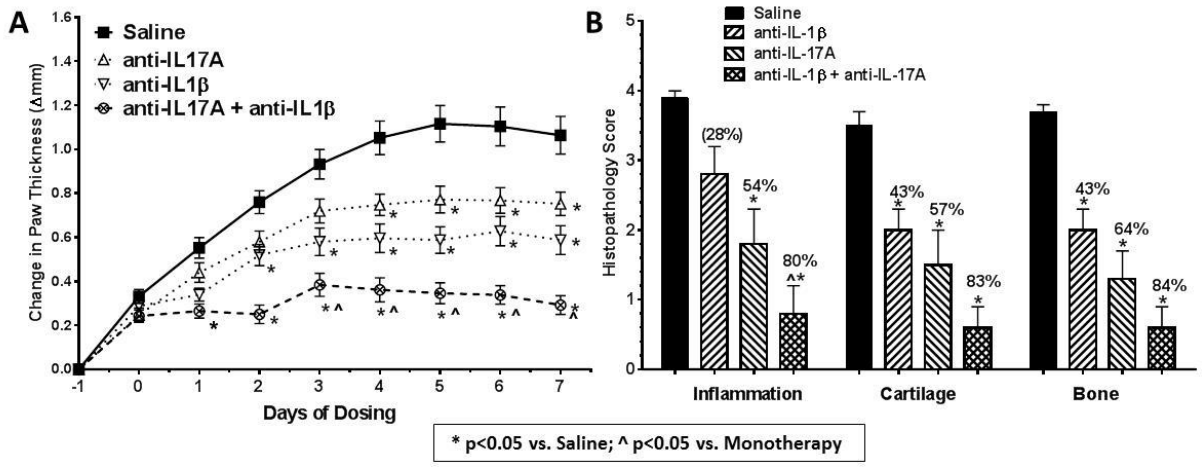

JPET Fast Forward. Published on January 8, 2018 as DOI: 10.1124/jpet.117.243493
This article has not been copyedited and formatted. The final version may differ from this version.

Figure 2.

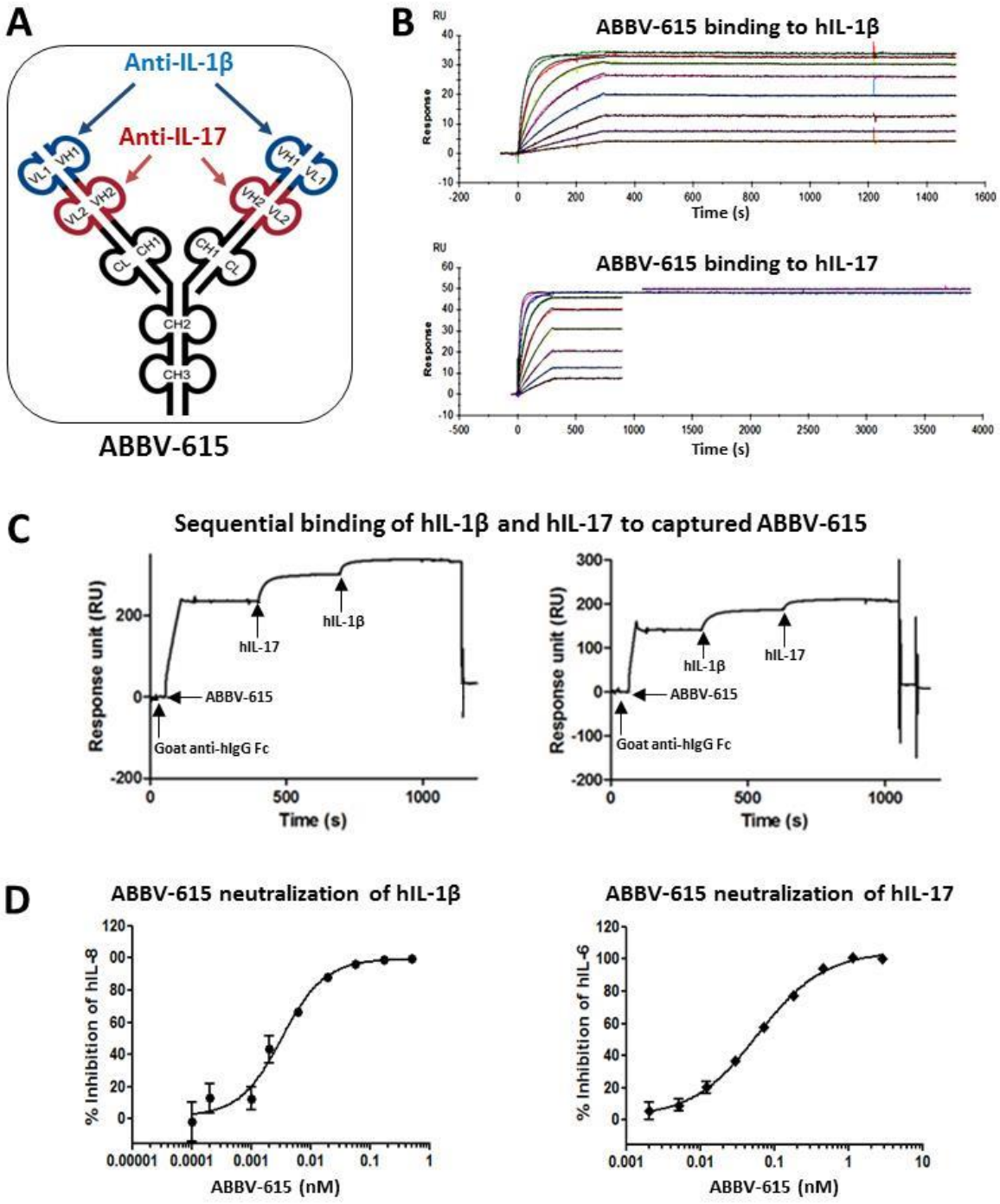

JPET Fast Forward. Published on January 8, 2018 as DOI: 10.1124/jpet.117.243493
This article has not been copyedited and formatted. The final version may differ from this version.

Figure 3.

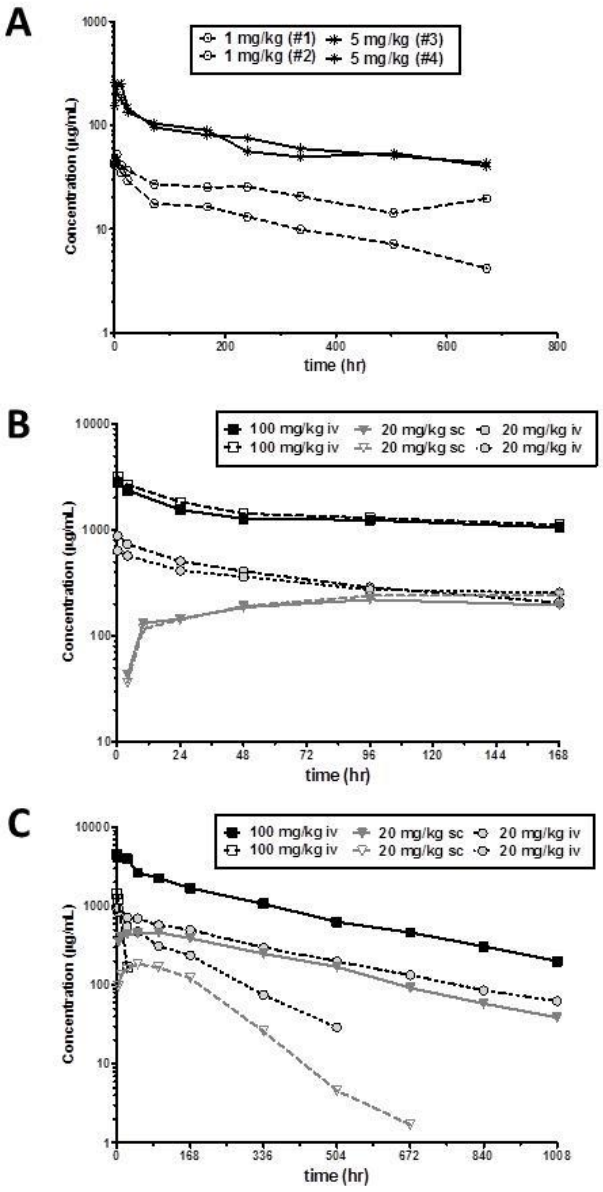

JPET Fast Forward. Published on January 8, 2018 as DOI: 10.1124/jpet.117.243493
This article has not been copyedited and formatted. The final version may differ from this version.

Figure 4.

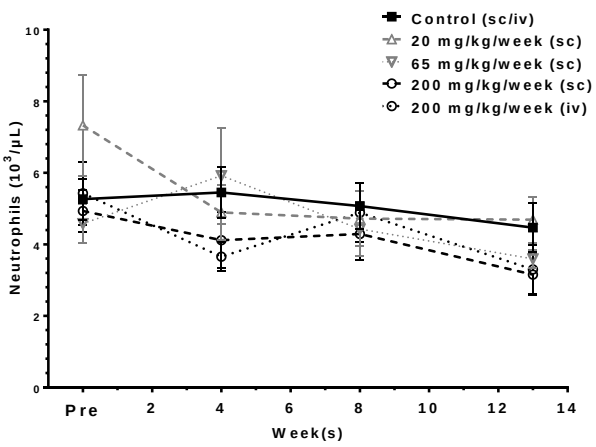

JPET Fast Forward. Published on January 8, 2018 as DOI: 10.1124/jpet.117.243493
This article has not been copyedited and formatted. The final version may differ from this version.

Figure 5.

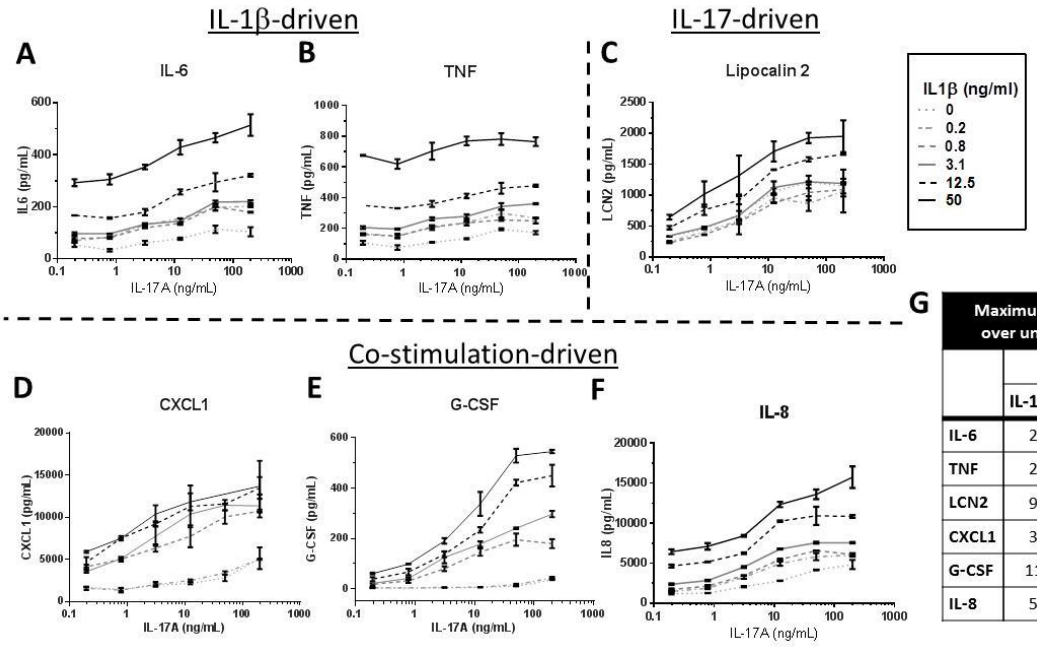

G

Maximum fold induction over untreated control			
	stimuli		
	IL-17A	IL-1β	Combo
IL-6	2	8	11
TNF	2	8	7
LCN2	9	3	15
CXCL1	3	3	8
G-CSF	11	6	162
IL-8	5	6	16

JPET Fast Forward. Published on January 8, 2018 as DOI: 10.1124/jpet.117.243493
This article has not been copyedited and formatted. The final version may differ from this version.

Figure 6.